



Contents lists available at ScienceDirect

Journal of Luminescence

journal homepage: www.elsevier.com/locate/jlumin

Analytical expressions for time-resolved optically stimulated luminescence experiments in quartz

V. Pagonis^{a,*}, J. Lawless^b, R. Chen^c, M.L. Chithambo^d

^a McDaniel College, Physics Department, Westminster, MD 21157, USA

^b Redwood Scientific Inc., Pacifica CA 94044, USA

^c Raymond and Beverly Sackler School of Physics and Astronomy, Tel-Aviv University, Tel-Aviv 69978, Israel

^d Department of Physics, Rhodes University, PO BOX 94, Grahamstown 6140, South Africa

ARTICLE INFO

Article history:

Received 25 January 2011

Received in revised form

15 April 2011

Accepted 20 April 2011

Available online 3 May 2011

Keywords:

Time resolved optically stimulated luminescence

TR-OSL

Pulsed luminescence

Quartz luminescence lifetimes

Thermal quenching

Kinetic model

ABSTRACT

Optically stimulated luminescence (OSL) signals can be obtained using a time-resolved optical stimulation (TR-OSL) method, also known as pulsed OSL. During TR-OSL measurements, the stimulation and emission of luminescence are experimentally separated in time using short light pulses. This paper presents analytical expressions for the TR-OSL intensity observed during and after such a pulse in quartz experiments. The analytical expressions are derived using a recently published kinetic model which describes thermal quenching phenomena in quartz samples. In addition, analytical expressions are derived for the concentration of electrons in the conduction band during and after the TR-OSL pulse, and for the maximum signals attained during optical stimulation of the samples. The relevance of the model for dosimetric applications is examined, by studying the dependence of the maximum TR-OSL signals on the degree of initial trap filling, and also on the probability of electron retrapping into the dosimetric trap. Analytical expressions are derived for two characteristic times of the TR-OSL mechanism; these times are the relaxation time for electrons in the conduction band, and the corresponding relaxation time for the radiative transition within the luminescence center. The former relaxation time is found to depend on several experimental parameters, while the latter relaxation time depends only on internal parameters characteristic of the recombination center. These differences between the two relaxation times can be explained by the presence of localized and delocalized transitions in the quartz sample. The analytical expressions in this paper are shown to be equivalent to previous analytical expressions derived using a different mathematical approach. A description of thermal quenching processes in quartz based on AlO_4^-/AlO_4 defects is presented, which illustrates the connection between the different descriptions of the luminescence process found in the literature.

© 2011 Elsevier B.V. All rights reserved.

1. Introduction—time resolved luminescence experiments in quartz

The technique of time-resolved optically stimulated luminescence (TR-OSL) is an important experimental tool for studying relaxation phenomena in a variety of materials. During the past decade, extensive TR-OSL measurements have been carried out using samples of both quartz and feldspars, due to the importance of these materials in dating and retrospective dosimetry applications ([1–8]). During TR-OSL measurements the stimulation is carried out with a brief light pulse, and photons are recorded based on their arrival at the luminescence detector with respect to the light pulse. Summing signals from several pulses gives rise to a typical TR-OSL curve that shows the buildup of luminescence

during the pulse and the subsequent decrease when the optical stimulation is turned off. The decaying luminescence signal immediately following any light pulse is commonly analyzed using the linear sum of exponential decays, and can therefore be characterized using decay constant(s) or luminescence lifetime(s). The main advantage of TR-OSL over continuous-wave optically stimulated luminescence (CW-OSL) measurements is that it allows study of recombination and/or relaxation pathways in the material, and therefore provides an important information on the underlying luminescence mechanisms.

Several researchers have studied the temperature dependence of luminescence lifetimes and luminescence intensity from time-resolved luminescence experiments in quartz (see for example, Refs. [9–13] and references therein). Luminescence lifetimes for unannealed sedimentary quartz are typically found to remain constant at $\sim 42 \mu\text{s}$ for stimulation temperatures between 20 and 100°C , and then to decrease continuously to $\sim 8 \mu\text{s}$ at 200°C . These phenomena are usually described within the framework of

* Corresponding author. Tel.: +410 857 2481; fax: +410 386 4624.
E-mail address: vpagonis@mcDaniel.edu (V. Pagonis).

thermal quenching of luminescence in quartz, which has been well-known for several decades. Thermal quenching has also been observed in both thermoluminescence (TL) and optically stimulated luminescence (OSL) experiments on quartz ([14,15]), and is commonly described using the Mott–Seitz mechanism (see for example Refs. [16–18], and references therein).

Recently Pagonis et al. [19] published a new kinetic model for thermal quenching in quartz, which is based on the Mott–Seitz mechanism. In this model all recombination transitions are localized within the recombination center (in contrast to delocalized models in which all charge transitions take place to or from the conduction and valence bands—e.g. Ref. [18]).

The purpose of this paper is to present analytical expressions for the luminescence intensity observed during and after the short pulses used during a TR-OSL experiment. These analytical expressions are obtained from the recent model of Pagonis et al. [19], by assuming that the traps are well below saturation. In addition, analytical expressions are derived for the concentration of electrons in the conduction band during and after the TR-OSL pulse, and for the maximum signals attained during optical stimulation of the samples. The relevance of the model for dosimetric applications is examined, by studying the dependence of the maximum TR-OSL signals on the degree of initial trap filling and on the probability of electron retrapping into the dosimetric trap. Finally, the expressions derived in this paper are shown to be equivalent to published analytical expressions previously derived using a completely different physical approach (Chithambo [12]).

2. Recent modeling of thermal quenching in quartz

Pagonis et al. [19] presented a numerical model for thermal quenching in quartz based on the Mott–Seitz mechanism. The model involves electronic transitions between energy states within the recombination center, and is used in this work to derive analytical expressions for the TR-OSL process in quartz. The Mott–Seitz mechanism is usually shown schematically using a configurational diagram as in Fig. 1a, and consists of an excited state of the recombination center and the corresponding ground state. In this mechanism, electrons are captured into an excited state of the recombination center, from which they can undergo either one of two competing transitions. The first transition is a direct radiative recombination route resulting in the emission of light and is shown as a vertical arrow in Fig. 1a. The second route is an indirect thermally assisted non-radiative transition into the ground state of the recombination center; the activation energy W for this non-radiative process is also shown in Fig. 1a. The energy given up in the non-radiative recombination is absorbed by the crystal as heat, rather than being emitted as photons. One of the main assumptions of the Mott–Seitz mechanism is that the radiative and non-radiative processes compete within the confines of the recombination center, hence they are referred to as localized transitions.

Fig. 1b shows the energy level diagram corresponding to the model. The arrows in Fig. 1b indicate the electronic transitions which are likely to be taking place during a typical TR-OSL experiment. This simplified model consists of an optically sensitive electron trap referred to in this paper as the dosimetric trap and shown as level 1, and several additional levels labeled 2–4 representing energy states within the recombination center. During the transition labeled 1, electrons from the dosimetric trap are raised by optical stimulation into the conduction band (CB), with some of these electrons being retrapped with a probability A_n as shown in transition 2. Transition 3 corresponds to an electronic transition from the CB into the excited state located below the conduction band, with probability A_{CB} . Transition 5 indicates the direct radiative transition from the excited

level into the ground electronic state with probability A_R , and transition 4 indicates the competing thermally assisted route. The probability for this competing thermally assisted process (transition 4) is given by a Boltzmann factor of the form $A_{NR} \exp(-W/k_B T)$, where W represents the activation energy for this process, and A_{NR} is a constant representing the non-radiative transition probability. Transition 6 denotes the non-radiative process into the ground state. The details of the non-radiative process in the model are not important for the purposes of this paper; what is critical in determining the thermal quenching effects is the ratio of the non-radiative and radiative probabilities A_{NR}/A_R and the value of the thermal activation energy W .

Thermal quenching within this model is caused by the competing transitions 4 and 5 in Fig. 1b. As the temperature of the sample is increased, electrons are removed from the excited state level 2 to the excited state level 3 according to the Boltzmann factor described above. This transition (level 2 → level 3) leads to both a decrease of the intensity of the luminescence signal, and to a simultaneous decrease of the luminescence lifetime with increasing stimulating temperature.

The parameters used in the model are defined as follows; N_1 is the total concentration of dosimetric traps (cm^{-3}), n_1 is the corresponding concentration of trapped electrons (cm^{-3}), N_2 is the total concentration of luminescence centers and $N_2 - n_2$ is the corresponding concentration of activated luminescence centers (cm^{-3}). A detailed discussion of the connection between the electronic concentrations n_2 , $N_2 - n_2$, N_2 and the concentrations of specific defects in quartz is presented in Section 6 of this paper.

$W=0.64$ eV is the activation energy for the thermally assisted process (eV), A_n is the conduction band to dosimetric electron trap transition probability coefficient ($\text{cm}^3 \text{s}^{-1}$), A_R and A_{NR} are the radiative and non-radiative transition probability coefficients (s^{-1}), respectively, and A_{CB} is the transition probability coefficient ($\text{cm}^3 \text{s}^{-1}$) for the conduction band to excited state transition. The parameter n_c represents the instantaneous concentration of electrons in the conduction band (cm^{-3}) and P denotes the probability of optical excitation of electrons from the dosimetric trap (s^{-1}).

The equations used in the model are as follows:

$$\frac{dn_1}{dt} = n_c(N_1 - n_1)A_n - n_1P, \quad (1)$$

$$\frac{dn_c}{dt} = -n_c(N_1 - n_1)A_n + n_1P - A_{CB}n_c(N_2 - n_2), \quad (2)$$

$$\frac{dn_2}{dt} = A_{CB}n_c(N_2 - n_2) - A_Rn_2 - n_2A_{NR}\exp(-W/k_B T). \quad (3)$$

The instantaneous luminescence $I(t)$ resulting from the radiative transition is defined as

$$I(t) = A_Rn_2. \quad (4)$$

It is noted that transitions 4, 5 and 6 in Fig. 1b are of a localized nature, while transition 3 involves electrons in the CB and hence is of a delocalized nature. The difference in the nature of these transitions can also be seen in their mathematical forms in Eqs. (1)–(4). The term $A_{CB}n_c(N_2 - n_2)$ in Eqs. (2) and (3) expresses the fact that there are $N_2 - n_2$ empty electronic states available for electrons in the CB; these are excited states of the recombination center, in agreement with the general assumptions of the Mott–Seitz mechanism of thermal quenching.

The values of the parameters used in the model of Pagonis et al. [19] are as follows:

$A_n=5 \times 10^{-10} \text{ cm}^3 \text{ s}^{-1}$, $A_R=1/42 \text{ } \mu\text{s}=2.38 \times 10^4 \text{ s}^{-1}$, $A_{CB}=10^{-8} \text{ cm}^3 \text{ s}^{-1}$, $P=0.2 \text{ s}^{-1}$, $A_{NR}=1.3 \times 10^{11} \text{ s}^{-1}$, $N_1=10^{14} \text{ cm}^{-3}$, $N_2=10^{14} \text{ cm}^{-3}$, and $W=0.64$ eV. The initial conditions for the different concentrations in the model are taken as: $n_1(0)=9 \times 10^{13} \text{ cm}^{-3}$, $n_2(0)=0$, $n_c(0)=0$.

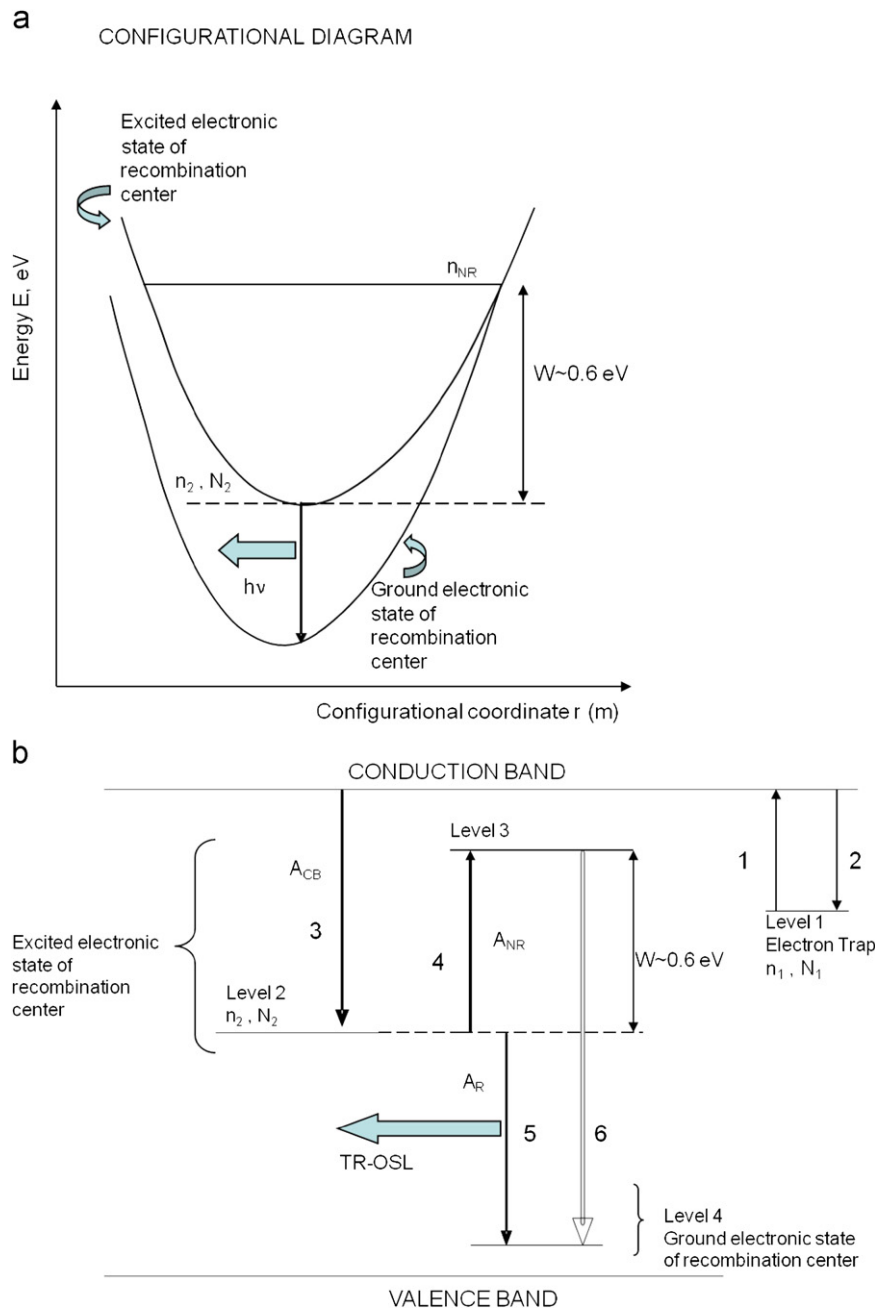


Fig. 1. (a) Configurational diagram for quartz, based on the Mott–Seitz mechanism of thermal quenching and (b) kinetic model of Pagonis et al. [19] for thermal quenching in quartz, based on the Mott–Seitz mechanism.

The value of the delocalized transition probability A_{CB} was chosen in the model of Pagonis et al. [19], so that the conduction band empties quickly during the TR-OSL experiment after the optical stimulation is turned off, on a time scale of $\sim 1 \mu\text{s}$. On the other hand, the value of the radiative transition probability $A_R = 1/42 \mu\text{s} = 2.38 \times 10^4 \text{ s}^{-1}$ was chosen so that the excited states (n_2) empty much slower during the TR-OSL experiment, and also so that it corresponds to the experimentally observed quartz luminescence lifetime of $\tau = 42 \mu\text{s}$ at room temperature.

3. Derivation of the analytical expressions

In this section it is shown that the system of Eqs. (1)–(4) can be solved analytically by assuming that the electron traps (levels

1 and 2 in Fig. 1b), are away from saturation. No other assumptions or approximations are necessary for deriving these analytical equations within the model. Analytical expressions will be derived for the luminescence intensity $I(t)$ and for the concentrations $n_2(t)$ and $n_c(t)$ during and after the TR-OSL pulse.

3.1. Analytical expressions for the electron concentration $n_c(t)$

We begin by deriving analytical equations for the concentration of electrons $n_c(t)$ in the CB as a function of time. During a TR-OSL experiment it is assumed that a small number of electrons are raised into the CB by optical excitation of the dosimetric trap. It is then reasonable to assume that during and after a TR-OSL pulse, the concentration of electrons in the dosimetric trap $n_1(t)$ does not change significantly; one can then approximate $n_1(t) \approx n_1(0)$,

where $n_1(0)$ is the value of $n_1(t)$ at the beginning of the TR-OSL experiment. We further assume that both electron traps n_1 and n_2 are far from saturation, i.e. $n_2 \ll N_2$ and $n_1 \ll N_1$. With these reasonable physical assumptions, Eq. (2) yields:

$$\begin{aligned} \frac{dn_c}{dt} &= -n_c(N_1 - n_1)A_n + n_1P - A_{CB}n_c(N_2 - n_2) \\ &\approx -n_c(N_1 - n_1(0))A_n + n_1(0)P - A_{CB}n_cN_2. \end{aligned} \quad (5)$$

This can be rearranged to yield a first order differential equation for $n_c(t)$:

$$\frac{dn_c}{dt} = -n_c[A_n(N_1 - n_1(0)) + A_{CB}N_2] + n_1(0)P. \quad (6)$$

The solution of this first order equation is given by:

$$\begin{aligned} n_c(t) &= \frac{n_1(0)P}{A_n(N_1 - n_1(0)) + A_{CB}N_2} \left(1 - e^{-[A_n(N_1 - n_1(0)) + A_{CB}N_2]t} \right) \\ &\text{for } 0 < t < t_o \text{ (during pulse),} \end{aligned} \quad (7)$$

where t_o represents the pulse width. Eq. (7) tells us that during a TR-OSL pulse the concentration of electrons n_c in the CB will grow exponentially, and will reach an equilibrium value. The characteristic time τ_{nc} for the increasing concentration $n_c(t)$ during the pulse is found by inspection of Eq. (7), and is given by:

$$\tau_{nc} = \frac{1}{A_n(N_1 - n_1(0)) + A_{CB}N_2}. \quad (8)$$

This characteristic time τ_{nc} depends on the parameters A_n , N_1 , $n_1(0)$, N_2 and A_{CB} in the model; this is discussed in some detail in a subsequent section of the paper. The equilibrium value $(n_c)_{EQ}$ reached by n_c during the TR-OSL pulse, is found by setting $t \rightarrow \infty$ in Eq. (7) to obtain the following expression:

$$(n_c)_{EQ} \sim \frac{n_1(0)P}{A_n(N_1 - n_1(0)) + A_{CB}N_2}. \quad (9)$$

This equilibrium value of n_c will be reached within a time interval of ~ 5 characteristic times τ_{nc} , and n_c will remain constant after this initial transient time. As mentioned previously, the values of the parameters in the model of Pagonis et al. [19] were chosen so that this characteristic time has a value of $\tau_{nc} = 1/[A_n(N_1 - n_1(0)) + A_{CB}N_2] = 1 \mu\text{s}$. The equilibrium value of $(n_c)_{EQ}$ in Eq. (9) depends on the parameters P , A_n , N_1 , $n_1(0)$, N_2 and A_{CB} in the model; this is also discussed later in this paper.

The corresponding solution $n_c(t)$ after the end of the optical stimulation, i.e. when the LED is turned OFF, is obtained by setting $P=0$ into Eq. (6) to obtain:

$$\frac{dn_c}{dt} = -n_c[A_n(N_1 - n_1(0)) + A_{CB}N_2]. \quad (10)$$

The solution of this equation is a simple decaying exponential of the form:

$$n_c(t) = n_c(t_o)e^{-[A_n(N_1 - n_1(0)) + A_{CB}N_2](t - t_o)} \quad \text{for } t > t_o \text{ (after pulse),} \quad (11)$$

where $n_c(t_o)$ represents the concentration n_c at the end of the TR-OSL pulse of duration t_o . The value $n_c(t_o)$ can be obtained easily from Eq. (7) by setting $t=t_o$. Eq. (11) shows that the concentration $n_c(t)$ after the end of the optical stimulation will decay with the same characteristic time τ_{nc} given by Eq. (8).

Eqs. (7) and (11) express the time variation of the concentration of electrons in the CB during and after the short optical stimulation pulse, respectively. These concentrations $n_c(t)$ can in principle be measured simultaneously with the intensity of the TR-OSL signal, by recording the optically stimulated conductivity of the quartz sample. Although such TR-OSL conductivity measurements have not been reported in the literature for quartz, the results of the model suggest that their measurement could provide important information for the charge movement in quartz samples.

3.2. Analytical expressions for the electron concentration $n_2(t)$

One can also obtain analytical expressions for the concentration $n_2(t)$ of electrons in the excited state of the recombination center, as follows. As discussed above, after a short initial time interval of the order of $\sim 1 \mu\text{s}$, the concentration of electrons in the CB during the optical stimulation will remain constant, and equal to the quasistatic equilibrium value $(n_c)_{EQ}$ given by Eq. (9). By substituting the constant value $(n_c)_{EQ}$ from Eq. (9) into Eq. (3) and using $n_2 \ll N_2$, one obtains:

$$\begin{aligned} \frac{dn_2}{dt} &= A_{CB}n_c(N_2 - n_2) - n_2(A_R + A_{NR}\exp(-W/kT)) \\ &\approx \frac{n_1(0)PA_{CB}N_2}{A_n(N_1 - n_1(0)) + A_{CB}N_2} - n_2(A_R + A_{NR}\exp(-W/kT)) \\ &= f - n_2(A_R + A_{NR}\exp(-W/kT)), \end{aligned} \quad (12)$$

where the constant f is defined by:

$$f = \frac{n_1(0)PA_{CB}N_2}{A_n(N_1 - n_1(0)) + A_{CB}N_2}. \quad (13)$$

The solution of the first order differential Eq. (12) is a saturating exponential of the form:

$$\begin{aligned} n_2(t) &= \frac{f}{A_R + A_{NR}\exp(-W/kT)} (1 - e^{-[A_R + A_{NR}\exp(-W/kT)]t}) \\ &\text{for } 0 < t < t_o \text{ (during pulse),} \end{aligned} \quad (14)$$

where t_o represents the pulse width.

The corresponding solution $n_2(t)$ after the end of the light pulse, i.e. when the LED is turned OFF, is obtained by setting $P=0$ and $f=0$ into Eq. (12) to obtain:

$$\frac{dn_2}{dt} = -n_2(A_R + A_{NR}\exp(-W/kT)). \quad (15)$$

The solution of this equation is a simple decaying exponential of the form:

$$n_2(t) = n_2(t_o)e^{-[A_R + A_{NR}\exp(-W/kT)](t - t_o)} \quad \text{for } t > t_o \text{ (after pulse),} \quad (16)$$

where as previously t_o is the pulse width, and $n_2(t_o)$ represents the concentration of n_2 at the end of the TR-OSL pulse. Eqs. (14) and (16) are the desired analytical expressions for the concentration $n_2(t)$ during and after the short optical pulse.

3.3. Analytical expressions for the luminescence intensity $I(t)$

By combining Eqs. (4), (14) and (16) we obtain analytical expressions for the luminescence intensity $I(t)$ measured during and after the TR-OSL pulse:

$$\begin{aligned} I(t) &= A_R \frac{f}{A_R + A_{NR}\exp(-W/kT)} (1 - e^{-[A_R + A_{NR}\exp(-W/kT)]t}) \\ &\text{for } 0 < t < t_o \text{ (during pulse),} \end{aligned} \quad (17)$$

$$\begin{aligned} I(t) &= A_R n_2(t_o) e^{-[A_R + A_{NR}\exp(-W/kT)](t - t_o)} \\ &\text{for } t > t_o \text{ (after pulse).} \end{aligned} \quad (18)$$

Eqs. (17) and (18) express the time-dependence of the luminescence intensity during the two stages of the TR-OSL experiment. These two equations agree with experimental results showing that the TR-OSL intensity for quartz during the stimulating light pulse can be described as a saturating exponential, while $I(t)$ after the stimulation light pulse is found to be a decaying simple exponential function.

From Eq. (17) we can find the maximum intensity I_{max} reached by the luminescence signal during the optical stimulations by setting $t \rightarrow \infty$:

$$I_{max} = A_R \frac{f}{A_R + A_{NR}\exp(-W/kT)}. \quad (19)$$

From Eqs. (17) and (18) we also find that the relaxation time for electrons from the excited into the ground state of the recombination center is:

$$\tau = \frac{1}{A_R + A_{NR} \exp(-W/kT)} = \frac{1/A_R}{1 + \frac{A_{NR}}{A_R} \exp(-W/kT)}. \quad (20)$$

This expression is of the same form as the following empirically derived equation for the luminescence lifetime of quartz as a function of the stimulation temperature T :

$$\tau = \frac{\tau_o}{1 + C \exp(-W/kT)}, \quad (21)$$

where τ_o is the experimental lifetime for the radiative recombination process in the material at low temperatures, and C is an empirical dimensionless parameter. As the temperature T of the sample is increased during the optical stimulation, the lifetime $\tau(T)$ of the electrons decreases according to Eq. (20). By comparing Eqs. (20) and (21) we find that the luminescence lifetime at low temperatures is given by

$$\tau_o = \frac{1}{A_R} = \frac{1}{2.38 \times 10^4 \text{ s}^{-1}} = 42 \text{ } \mu\text{s} \quad (22)$$

and that the empirical dimensionless constant C is given by:

$$C = \frac{A_{NR}}{A_R} = \frac{1.3 \times 10^{11} \text{ s}^{-1}}{2.38 \times 10^4 \text{ s}^{-1}} = 0.55 \times 10^7. \quad (23)$$

The expression in Eq. (23) for the empirical constant C is also consistent with the original Mott–Seitz formulation, in which C represents the ratio of non-radiative probability A_{NR} over the radiative recombination probability A_R (see the discussion in Pagonis et al. [19]). It should also be noted that in some previous studies (e.g. Chithambo [12], Akselrod et al. [20]), the parameter C was expressed as a product of two parameters ν and τ_R , i.e. $C = \nu \tau_R$. In these previous studies ν was defined as the frequency factor applicable to the non-radiative process and τ_R as the radiative lifetime at absolute zero. This previous description is consistent with the formulation in Eq. (23), where the corresponding parameters can now be identified as $\nu = A_{NR}$ and $\tau_R = 1/A_R$.

Another physical result from the model can be found by inspection of Eq. (19), in which the maximum intensity during the optical pulse is found to be:

$$I_{max} = A_R \frac{f}{A_R + A_{NR} \exp(-W/kT)} = \frac{f}{1 + (A_{NR}/A_R) \exp(-W/kT)} = \frac{f}{1 + C \exp(-W/kT)}. \quad (24)$$

This expression is of the same form as the following empirically derived equation for the maximum luminescence intensity as a function of the stimulation temperature T :

$$I_{max} = \frac{I_o}{1 + C \exp(-W/kT)}, \quad (25)$$

where I_o is the experimental luminescence at low temperatures (see for example Ref. [19]). As the stimulation temperature T of the sample is increased during the optical stimulation, the maximum intensity I_{max} decreases according to Eq. (25).

4. Comparison of analytical expressions and simulated results

The calculated values of $I(t)$ and $n_c(t)$ using the analytical expressions (7), (11), (17) and (18) are shown in Fig. 2, together with the exact numerical solutions of the system of Eqs. (1)–(4). The agreement between the analytical and numerical solutions in Fig. 2 can be seen to be very good. One can also check numerically the quasistatic equilibrium values reached by the various concentrations during the TR-OSL experiment. The quasistatic equilibrium

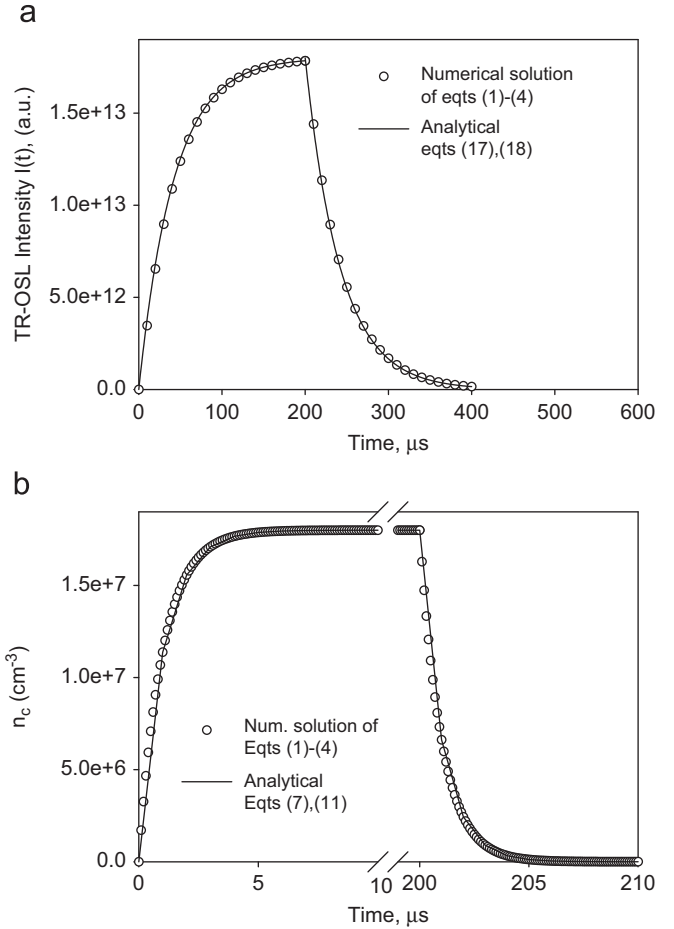


Fig. 2. Simulated results for (a) the luminescence intensity $I(t)$ and (b) the concentration $n_c(t)$ of electrons in the conduction band, during and after a TR-OSL pulse. The analytical expressions (7), (11), (17) and (18) are shown together with the exact numerical solutions of the system of Eqs. (1)–(4). The agreement between the analytical and numerical solutions can be seen to be very good. A break is introduced on the time-axis, so that the details of the graph can be better seen.

value for free electrons in the conduction band is given by Eq. (9):

$$(n_c)_{EQ} \sim \frac{n_1(0)P}{A_n(N_1 - n_1(0)) + A_{CB}N_2} = 1.8 \times 10^7 \text{ cm}^{-3}. \quad (26)$$

This equilibrium value of n_c is in close agreement with the values shown in Fig. 2b.

Similarly, the asymptotic luminescence I_{max} reached by the luminescence signal $I(t)$ can be found from Eq. (24):

$$I_{max} = A_R \frac{f}{A_R + A_{NR} \exp(-W/kT)}. \quad (27)$$

At room temperature the term $A_{NR} \exp(-W/kT)$ is negligible compared to the probability A_R , and this equation combined with Eq. (13) gives

$$(I_{max})_{RT} \approx f = \frac{n_1(0)PA_{CB}N_2}{A_n(N_1 - n_1(0)) + A_{CB}N_2}. \quad (28)$$

By inserting the numerical values of the parameters we find

$$(I_{max})_{RT} \approx f = 1.8 \times 10^{13} \text{ cm}^{-3}. \quad (29)$$

This asymptotic value of the intensity is in close agreement with the value shown in Fig. 2a.

4.1. Discussion of Eq. (8)

It is also instructive to examine how the characteristic time τ_{nc} in Eq. (8) depends on the parameters of the model, namely parameters $A_n, N_1, n_1(0), N_2$ and A_{CB} . On the basis of the numerical values of these parameters used in Pagonis et al. [19], the retrapping term $n_c(N_1 - n_1)A_n$ in Eq. (1) is much smaller than the optical excitation term n_1P in the same equation. Under these conditions Eq. (8) can be approximated as:

$$\tau_{nc} \approx \frac{1}{A_{CB}N_2}. \tag{30}$$

This equation indicates that the characteristic time τ_{nc} for electrons in the conduction band will be inversely proportional to the total concentration of recombination centers N_2 in the sample. We have carried out simulations by varying the value of N_2 , while all other parameters in the model are kept fixed. The results of these simulations are shown in Fig. 3, in which the concentration $n_c(t)$ after the end of the optical stimulation is plotted for several values of N_2 . As the value of N_2 is increased, the concentration $n_c(t)$ can be seen in Fig. 3 to decay faster. The inset of Fig. 3 shows the characteristic time τ_{nc} obtained by fitting exponential decay curves to the simulated data. The dashed line in the inset shows the values of τ_{nc} calculated from Eq. (8), showing a very good agreement between the simulations and the analytical equation.

4.2. The effect of retrapping: simulations varying the initial concentration of dosimetric traps $n_1(0)$

From an experimental point of view, the easiest controllable parameter is the initial concentration of electrons in the dosimetric trap $n_1(0)$. The value of $n_1(0)$ clearly depends on the irradiation and thermal history of the sample. For a freshly annealed and irradiated sample, the value of $n_1(0)$ is in many situations proportional to the irradiation dose D received by the freshly annealed sample immediately before the TR-OSL experiment. As seen in Eqs. (8) and (28), the value of the initial concentration of electrons in the dosimetric trap $n_1(0)$ will affect two quantities which can be evaluated experimentally, namely

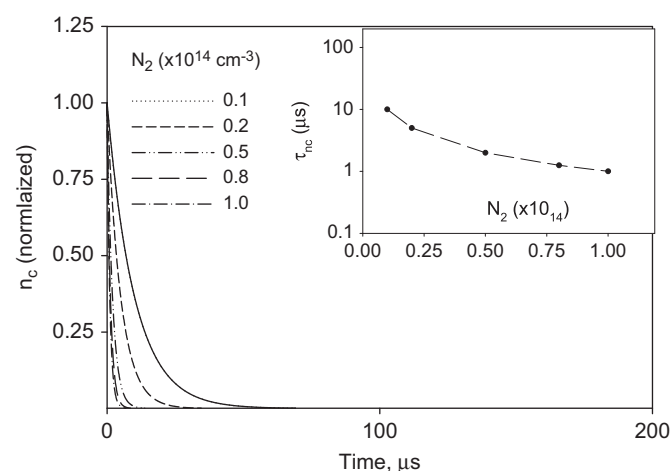


Fig. 3. Simulations of TR-OSL experiments, by varying the value of the total concentration of recombination centers N_2 , while all other parameters in the model of Pagonis et al. [19] are kept fixed. The concentration $n_c(t)$ after the end of the optical stimulation is plotted for several values of N_2 . As the value of N_2 is increased, the concentration $n_c(t)$ can be seen to decay faster. The inset shows the characteristic time τ_{nc} obtained by fitting exponential decay curves to the simulated $n_c(t)$ curves in the figure. The dashed line in the inset shows the values of τ_{nc} calculated from Eq. (8), showing a very good agreement between the simulations and the analytical expression.

the maximum TR-OSL intensity I_{max} , and the characteristic lifetime τ_{nc} for electrons in the conduction band.

Two different cases are considered next, depending on the value of the probability A_n of electron retrapping from the conduction band into the dosimetric trap.

4.2.1. Case #1: negligible retrapping in the dosimetric trap

We have carried out simulations by varying the degree of trap filling of the dosimetric trap, which is expressed by the ratio $n_1(0)/N_1$. During these simulations, all parameters are kept fixed as previously, and the value of $n_1(0)/N_1$ is varied from 0 (empty dosimetric traps) to 1 (completely filled traps). The results from the simulations are shown as solid circles in Fig. 4, using the original values of the parameters in the model of Pagonis et al. [19].

In the case of quartz samples, the numerical values in the model are such that the retrapping term $n_c(N_1 - n_1)A_n$ in Eq. (1) is much smaller than the optical excitation term n_1P in the same equation. Under these conditions the maximum intensity of the TR-OSL signal during the optical stimulation at room temperature will be found from Eq. (28), by dropping the term $A_n(N_1 - n_1(0))$ in the denominator:

$$(I_{max})_{RT} = \frac{n_1(0)PA_{CB}N_2}{A_n(N_1 - n_1(0)) + A_{CB}N_2} \approx n_1(0)P. \tag{31}$$

This equation tells us that within the parameters of the current model, the maximum intensity I_{max} will be strictly proportional to the initial concentration of electrons in the dosimetric trap $n_1(0)$, and will also be independent of the concentrations N_1 and N_2 . Therefore any experimentally observed deviations of I_{max} from linearity with the irradiation dose, could be indicative of strong retrapping of electrons from the conduction band into the dosimetric trap. The case of strong retrapping is discussed next.

4.2.2. Case #2: strong retrapping into the dosimetric trap

While the effect of retrapping may be very small for quartz samples for most cases, it may be significant for other materials in which the retrapping term $n_c(N_1 - n_1)A_n$ becomes comparable in magnitude to the optical excitation term n_1P in Eq. (1). An example of simulated I_{max} vs. the trap occupancy $n_1(0)$ is shown as open circles and triangles in Fig. 4. The parameters in the simulation of Fig. 4 are such that the retrapping probability A_n is allowed to vary over several orders of magnitude, from its initial

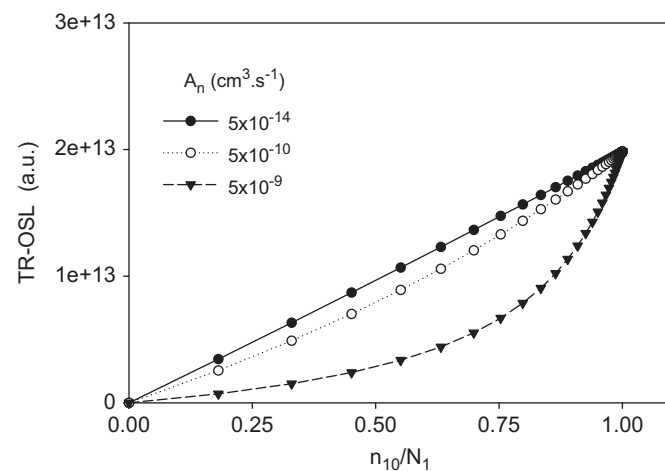


Fig. 4. Examples of simulated maximum luminescence intensity I_{max} , for different values of the trap occupancy $n_1(0)/N_1$. The solid circles are obtained using the parameters in the model of Pagonis et al. [19]. The open circles and triangles are obtained using much larger values of the retrapping probability A_n . The simulated results show that in the case of strong retrapping, a nonlinear behavior of I_{max} is observed as a function of the trap occupancy $n_1(0)/N_1$.

value of $A_n = 5 \times 10^{-14} \text{ cm}^3\text{s}^{-1}$, up to a value of $A_n = 5 \times 10^{-8} \text{ cm}^3\text{s}^{-1}$. The simulated results of Fig. 4 show that in the case of strong retrapping, a nonlinear behavior of I_{max} is observed as a function of the trap occupancy $n_1(0)$.

When the dosimetric trap is completely filled at the beginning of the TR-OSL experiment ($n_{10}/N_1 = 1$), Eq. (31) indicates that the value of I_{max} is equal to $(I_{max})_{RT} = n_1(0)P$, independently of the amount of retrapping. This is in agreement with the simulated results in Fig. 4, in which the three simulated curves converge at the point $n_{10}/N_1 = 1$.

The presence of retrapping will also affect the relaxation time of the concentration $n_c(t)$. In Fig. 5 we show this concentration $n_c(t)$ as a function time, for different degrees of initial trap filling $n_1(0)/N_1$. The inset of Fig. 5 shows the characteristic time τ_{nc} calculated from fitting decaying exponentials to this simulated data. As the value of the ratio $n_1(0)/N_1$ is increased, $n_c(t)$ can be seen to decay slower with time, and the corresponding time τ_{nc} increases from $\sim 0.5 \mu\text{s}$ for almost empty traps, to a value of $\sim 1 \mu\text{s}$ for completely filled traps.

In general, the total concentrations N_1 and N_2 appearing in the analytical equations in this paper will also be sample dependent, and they are physical characteristics of the dosimetric trap and of the recombination center correspondingly. One would therefore expect that these total concentrations depend on the type of quartz samples under consideration. For example, the concentration of recombination centers N_2 will also depend on the thermal annealing history of the sample. Specifically as a quartz sample is annealed gradually from room temperature to high temperatures above 600°C , the value of N_2 most likely will decrease with the annealing temperature, due to a redistribution of holes among the multiple recombination centers known to exist in quartz (see for example the discussion in Refs. [9,21,22]).

The results in this section were concerned with the dependence the maximum TR-OSL on the trap occupancy, rather than with the dose received by the sample. However the trap occupancy may not be linear with dose, and in fact can be expected to reach saturation at high doses. The overall dependence of the TR-OSL signal on the dose will arise from the combined effect of these two dependencies.

In this section we investigated the “maximum TR-OSL intensity” as measured during a TR-OSL experiment involving single stimulation pulses. The situation will be very different in the case of time-resolved measurements made using pulses separated by

intervals shorter than the luminescence lifetimes. Such experiments are usually termed pulsed OSL (POSL), and their mathematical description will be different than the model presented here.

5. Comparison with the model by Chithambo [12]

It is instructive to compare the model in this paper with the recent model of Chithambo [12]. In this section it will be shown that the two approaches yield almost identical results, even though they are derived using rather different approaches.

Chithambo [12] developed a general analytical model for time-resolved luminescence consisting of one electron-trapping state and one type of recombination center, with electronic transitions taking place from the trap to the center via the conduction band. The model is formulated in very general terms, by describing the rate of change of the number of stimulated electrons N by the differential equation:

$$\frac{dN}{dt} = sA - \lambda N, \tag{32}$$

where A represents the initial electron population, s is the probability of stimulation per unit time, and λ is the decay constant representing the probability per unit time that a stimulated electron will produce luminescence. This general differential equation can be compared directly with Eq. (12) derived in this paper:

$$\frac{dn_2}{dt} = \frac{n_1(0)PA_{CB}N_2}{A_n(N_1 - n_1(0)) + A_{CB}N_2} - n_2(A_R + A_{NR}\exp(-W/kT)). \tag{12}$$

By assuming small retrapping probability $A_n(N_1 - n_1(0)) \ll A_{CB}N_2$, this equation becomes:

$$\frac{dn_2}{dt} = n_1(0)P - n_2(A_R + A_{NR}\exp(-W/kT)). \tag{33}$$

The constants A and s in Eq. (32) correspond to $n_1(0)P$ in Eq. (33) correspondingly, while the decay constant $\lambda = 1/\tau$ can be identified with the luminescence probability per unit time, $A_R + A_{NR}\exp(-W/kT)$:

$$\lambda = 1/\tau = A_R + A_{NR}\exp(-W/kT). \tag{34}$$

This equation leads to the decay time as a function of the stimulation temperature T :

$$\tau = 1/\lambda = \frac{1}{A_R + A_{NR}\exp(-W/kT)} = \frac{1/A_R}{1 + \frac{A_{NR}}{A_R}\exp(-W/kT)}, \tag{35}$$

which is identical to Eq. (20) derived using the model in this paper. We conclude that the very general formulation by Chithambo [12] leads to identical results as the model in this paper, although the two physical approaches are very different.

6. Comparison of three commonly used descriptions of the luminescence process in quartz

In this section we compare and contrast three commonly used descriptions of the luminescence process in quartz. Specifically we discuss some of the defects which are believed to act as recombination centers in quartz, and address the relationship between the localized and delocalized transitions contained in these three commonly used types of descriptions.

Firstly, we present a general physical description of the luminescence process based on some of the ionic defects believed to act as luminescence centers in quartz. Secondly, we discuss a commonly used description of the luminescence process in quartz in terms of holes and delocalized transitions involving the conduction band. Thirdly, we discuss the equivalent description of the same luminescence process in terms of electronic states and

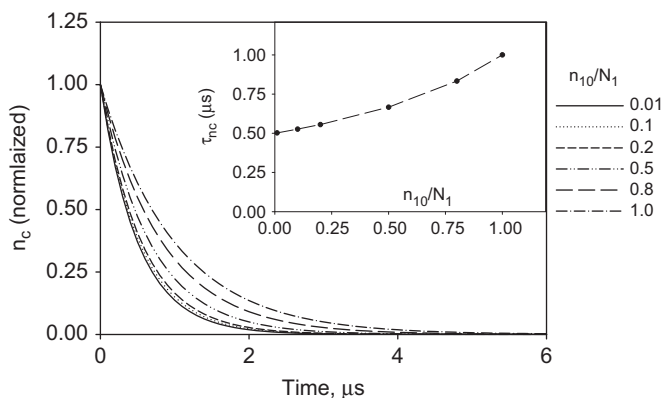


Fig. 5. Effect of retrapping on the concentration $n_c(t)$ observed after the end of the optical stimulation. The concentration $n_c(t)$ is shown as a function of the degree of trap filling $n_1(0)/N_1$. The simulated data are normalized to the first point on the graph. The inset shows the characteristic time τ_{nc} calculated from fitting decaying exponentials to the simulated $n_c(t)$ curves. As the degree of initial trap filling $n_1(0)/N_1$ is increased, $n_c(t)$ can be seen to decay slower with time, with the corresponding times increasing from $\sim 0.5 \mu\text{s}$ for almost empty traps, up to a value of $\sim 1 \mu\text{s}$ for completely filled traps.

localized transitions; this latter type of description is used in the present paper. Finally, the relationship between the three descriptions is discussed and the analogies between their mathematical and physical quantities are pointed out.

The luminescence process in quartz is known to be extremely complex, and several experimental studies have attempted to correlate specific defects with the experimentally observed luminescence emission in this material. For a complete review of the luminescence properties of quartz including an extensive list of references, the reader is referred to the recent paper by Preusser et al. [23].

In this paper we will discuss one specific example of the luminescence mechanism in quartz which involves the ionic center AlO_4^- which can act as a recombination center. The relevant physical process creating the luminescence defect in quartz involves Al_3^+ ions, which are known to act as a substitutional ion in quartz, replacing Si^{4+} . This substitutional process results in a positive hole which is trapped in the vicinity of the Al ion. Several experimental studies have identified the primary role played by this ionic complex in the luminescence properties of quartz [23]. For example, it has been suggested that the well-known 380 nm emission in quartz is likely the result of recombination processes taking place at these ionic complexes.

7. Description of the luminescence process in quartz in terms of point defects

In completely general terms, all luminescent solids contain luminescent ions (or complexes) that we call centers, and luminescence studies are interested in two versions or states of these centers. Researchers commonly identify a version of these ions/complexes with their “normal” charge, as well as an ionized version of these complexes. A normal version becomes an ionized version by “capturing a hole”, or equivalently by losing an electron. An ionized version becomes a normal version of the complex by capturing an electron. Both versions of the ionic complexes have vibrational states, and either version may also have electronically excited states.

Specifically in the case of the 380 nm emission of quartz, the normal version of the luminescent complex is assumed to be AlO_4^- , and the ionized version of the luminescent complex is AlO_4 . During irradiation, AlO_4^- captures a hole (or equivalently releases an electron) and becomes AlO_4 , with the released electron becoming trapped elsewhere in an electron trap in the crystal. During a typical TR-OSL experiment, this trapped electron is optically stimulated out of the trap and recombines with AlO_4 , resulting in the creation of $(AlO_4^-)^*$, i.e. an excited state of AlO_4^- . The excited state $(AlO_4^-)^*$ relaxes into the ground state AlO_4^- by either photon emission or by a non-radiative transition. Schematically, the process of an electron in the conduction band being captured by a luminescence complex AlO_4 can be written as:



In the Mott–Seitz model of thermal quenching, $(AlO_4^-)^*$ may decay to the ground state of AlO_4^- through the two possible electronic transitions shown in Fig. 2 of this paper.

8. Mathematical description of the luminescence process using “holes”

There have been several published complex kinetic models which attempt to describe the luminescence process in quartz, using delocalized transitions involving the conduction band (see for example Refs. [18,19,24] and references therein). In such

models, the total concentration of the two versions of the luminescence complexes is commonly denoted by M . The corresponding concentration of the ionized version of the complex is denoted by m , and therefore the concentration of the normal version of the complexes is $M - m$. Hence in quartz models using this notation, the concentration of the luminescent complex AlO_4^- would be denoted by $M - m$, while the corresponding concentration of the ionized luminescent complex AlO_4 by m .

The concentration m is changed every time an electron combines with a trapped hole in the recombination center via the delocalized transition shown as A_{CB} in Fig. 1. The overall rate of change of the concentration of holes m in this mathematical description can therefore be expressed by:

$$\frac{dm}{dt} = -A_{CB}mn_c, \tag{37}$$

in the above notation. This is the common form of writing the rate of recombination processes, as used in kinetic models involving only delocalized transitions. In terms of the discussion in the previous subsection, the term $A_{CB}mn_c$ in Eq. (37) represents mathematically the rate of the electron capture process shown in Eq. (36).

This mathematical description of the luminescence process in quartz is based on the concept of holes with concentrations m , and uses solely delocalized transitions involving the conduction band. In such models the Mott–Seitz mechanism for thermal quenching is not given an explicit mathematical form, and no mathematical description is provided for the localized transitions taking place within the recombination complex. Thermal quenching effects are expressed instead as an overall empirical correction factor $\eta(T)$ multiplying the luminescence intensity. Specifically, in such a model the luminescence intensity $I(t)$ is commonly written in the form:

$$I(t) = -\frac{dm}{dt} = \eta(T)A_{CB}mn_c, \tag{38}$$

with the thermal quenching correction factor given by:

$$\eta(T) = \frac{1}{1 + C \exp(-W/kT)}. \tag{39}$$

The thermal quenching parameters C and W in this equation have the same meaning as in Eq. (25). Clearly this type of mathematical description is inadequate to describe time-resolved luminescence experiments in quartz, or the associated effect of thermal quenching on the luminescence lifetimes. However, such models do provide a description of the observed effect of thermal quenching on the overall luminescence intensity via Eq. (38).

9. Mathematical description of the luminescence process using electronic states

In the model presented in this paper, the luminescence process is described using electronic states, instead of the concept of holes used in the previous section. The present model offers a mathematical description of a completely internal mechanism within the luminescence complex, and is based on electronic transitions of a localized nature.

In the example of the 380 nm emission for quartz discussed here, this type of model addresses the behavior of electronically excited states of AlO_4^- . For example, level 2 in Fig. 1b of this paper would represent an electronically-excited state of AlO_4^- , denoted by $(AlO_4^-)^*$. In terms of the previous discussion based on defects, $(AlO_4^-)^*$ decays to the ground state of AlO_4^- through either a radiative transition or a non-radiative transition. This competition between radiative and non-radiative transitions within the

recombination complex $(AlO_4)^*$ results in thermal quenching effects in quartz.

Mathematically in this type of model the concentration of $(AlO_4)^*$ complexes in the sample is expressed by the concentration of electrons n_2 in Fig. 2. The corresponding concentration of AlO_4 ions will then be denoted by $N_2 - n_2$, and the total concentration of both possible states (AlO_4^- and AlO_4) will be N_2 .

In the model presented in this paper, the internal transitions occurring within the recombination complex are given a specific mathematical form involving the concentrations n_2 and $N_2 - n_2$ of the two types of complexes. It is clear that the mathematical analog of the transition rate $A_{CB}mn_c$ used in Eq. (37) will be $A_{CB}(N_2 - n_2)n_c$, as shown explicitly in Eq. (3).

Finally, we note the following mathematical correspondence between the concentration of holes m , the electronic concentration n_2 and the type of defect in quartz:

$$n_2 = M - m \quad (\text{concentration of } AlO_4^-),$$

$$N_2 - n_2 = m \quad (\text{concentration of } AlO_4),$$

$$N_2 = M \quad (\text{total concentration of both } AlO_4 \text{ and } AlO_4^-).$$

The luminescence process in quartz is known to be very complex, involving several types of defects acting as recombination centers, electron and/or hole traps, and perhaps in some cases acting as both. Hence the description presented in this paper is certainly a simplification of a very complex luminescence process. However, this specific example based on AlO_4^- and AlO_4 clarifies the connection between the different descriptions of the luminescence process found in the literature.

10. Conclusions

In this paper we have presented analytical expressions relevant to TR-OSL experiments in quartz. The analytical expressions are derived using a recently published kinetic model which describes thermal quenching phenomena in quartz samples, and are applicable both during and after the optically stimulating pulse. In addition, analytical expressions are derived for the concentration of electrons in the conduction band, and for the maximum intensity signals attained during optical stimulation of the samples.

Two characteristic times for the TR-OSL process can be studied using the analytical equations; these times are the relaxation time for electrons in the conduction band (τ_{nc}), as well as the relaxation time (τ) for the radiative transition within the luminescence center. The former relaxation time (τ_{nc}) depends on several experimentally dependent parameters, as shown in Eq. (8). However, the latter relaxation time (τ) depends only on the parameters A_R , A_{NR} and W , as shown in Eq. (20). The analytical expressions (8) and (20) for the two relaxation times clearly show that their fundamental difference lies in the fact that τ_{nc} describes a delocalized process taking place through the conduction band,

while τ describes a completely localized process within the recombination center.

The relevance of the model for dosimetric applications was shown by studying the dependence of the maximum TR-OSL signals on the degree of initial trap filling, and also on the probability of electron retrapping into the dosimetric trap. When retrapping into the dosimetric trap is small, linearity between the TR-OSL signal and the initial trap filling can be expected. This in turn may indicate that in the case of small retrapping, the TR-OSL signal can be expected to be linear with the irradiation dose. The analytical expressions in this paper are shown to be equivalent to previous analytical expressions derived using a different mathematical approach.

The description of thermal quenching processes in quartz presented in this paper is certainly a simplification, and the specific example provided here is based on AlO_4^-/AlO_4 defects. Other types of defects have also been proposed as possible recombination centers in quartz, however, the example presented in this paper illustrates the connection between the different descriptions of the luminescence process found in the literature.

References

- [1] D.C.W. Sanderson, R.J. Clark, *Radiat. Meas.* 23 (1994) 633.
- [2] I.K. Bailiff, *Radiat. Meas.* 32 (2000) 401.
- [3] S. Tsukamoto, P.M. Denby, A.S. Murray, L. Bøtter-Jensen, *Radiat. Meas.* 41 (2006) 790.
- [4] P.M. Denby, L. Bøtter-Jensen, A.S. Murray, K.J. Thomsen, P. Moska, *Radiat. Meas.* 41 (2006) 774.
- [5] M.L. Chithambo, F.O. Ogundare, J. Feathers, *Radiat. Meas.* 43 (2008) 1.
- [6] C. Ankjærgaard, M. Jain, R. Kalchgruber, T. Lapp, D. Klein, S.W.S. McKeever, A.S. Murray, P. Morthekei, *Radiat. Meas.* 44 (2009) 576.
- [7] V. Pagonis, S.M. Mian, M.L. Chithambo, E. Christensen, C.J. Barnold, *J. Phys. D: Appl. Phys.* 42 (2009) 055407.
- [8] C. Ankjærgaard, M. Jain, K.J. Thomsen, A.S. Murray, *Radiat. Meas.* 45 (2010) 778–785.
- [9] R.B. Galloway, *Radiat. Meas.* 35 (2002) 67.
- [10] M.L. Chithambo, *Radiat. Meas.* 37 (2003) 167.
- [11] M.L. Chithambo, *Radiat. Meas.* 41 (2006) 862.
- [12] M.L. Chithambo, *J. Phys. D: Appl. Phys.* 40 (2007) 1874.
- [13] M.L. Chithambo, *J. Phys. D: Appl. Phys.* 40 (2007) 1880.
- [14] B.W. Smith, E.J. Rhodes, S. Stokes, N.A. Spooner, *Radiat. Prot. Dosim.* 34 (1990) 75.
- [15] N.A. Spooner, *Radiat. Meas.* 23 (1994) 593.
- [16] L. Bøtter-Jensen, S.W.S. McKeever, A.G. Wintle, *Optically Stimulated Luminescence Dosimetry*, Amsterdam: Elsevier, 2003.
- [17] R. Chen, S.W.S. McKeever, *Theory of Thermoluminescence and Related Phenomena*, 1997, Singapore: World Scientific.
- [18] R.M. Bailey, *Radiat. Meas.* 33 (2001) 17.
- [19] V. Pagonis, C. Ankjærgaard, A.S. Murray, R. Chen, *J. Lumin.* 130 (2010) 902.
- [20] M.S. Akselrod, N. Agersnap Larsen, V. Whitley, S.W.S. McKeever, *J. Appl. Phys.* 84 (1998) 3364.
- [21] M.L. Chithambo, R.B. Galloway, *Nucl. Instrum. Meth. Phys. Res. B* 183 (2001) 358.
- [22] M.L. Chithambo, F.O. Ogundare, *Radiat. Meas.* 44 (2009) 453.
- [23] F. Preusser, M.L. Chithambo, T. Götze, M. Martini, K. Ramseyer, E.J. Sendezera, G.J. Susino, A.G. Wintle, *Earth-Sci. Rev.* 97 (2009) 196.
- [24] V. Pagonis, A.G. Wintle, R. Chen, X.L. Wang, *Radiat. Meas.* 43 (2008) 704.